ORAL/POSTER REFERENCE: ICF100936OR

# ANALYSIS OF SUBSONIC INTERFACIAL FRACTURE USING STRAIN GAGES IN AN ISOTROPIC-ORTHOTROPIC BIMATERIAL

Vittorio Ricci[1], Kwang Ho Lee[2], Arun Shukla[3], and Vijay Chalivendra[3]

[1] Naval Undersea Warfare Center Division, Newport, RI 02841, USA
[2] Sangju National University, Republic of Korea
[3] Department of Mechanical Engineering, University of Rhode Island, Kingston, RI 02881, USA

## ABSTRACT

An experimental study has been conducted in which strain fields were used to investigate the behavior of subsonic crack propagation along the interface of an isotropic-orthotropic bimaterial system. Strain field equations were developed from available field equations and critically evaluated in a parametric study to identify optimum strain gage location and orientation. Bimaterial specimens were prepared with PSM-1 polycarbonate and Scotchply® 1002 unidirectional, glass-fiber-reinforced, epoxy composite. Dynamic experiments were conducted using these specimens with strain gages mounted on the composite half to obtain values of the dynamic complex stress intensity factor (CSIF), $\mathbf{K^d} = K_1^d + iK_2^d$, in the region of the crack tip while photoelasticity was used on the PSM-1 half. Results show that the trend and magnitude of $\mathbf{K^d}$ obtained using strain gages compare favorably with those obtained using photoelasticity. Therefore, it is feasible to use strain gages to investigate interfacial crack propagation in isotropic-orthotropic bimaterials.

## KEYWORDS

Strain gages, bimaterials, interface, orthotropic, fracture, subsonic crack propagation

## INTRODUCTION

Because of their low cost and ease of use, the strain gage remains the predominant measuring device in industry. Thus, the development of strain gage techniques in bimaterial problems would greatly facilitate the analysis of such problems for practical application. Strain gage methods have been used in fracture research conducted on isotropic materials [1,2] and in orthotropic materials [3,4]. Substantial progress has been made in the study of dynamic interfacial fracture. Yang *et al.* [5] provided the asymptotic structure of the most singular term of the steady-state elastodynamic interfacial crack-tip fields. Deng [6,7] obtained a complete series solution for the stress field around a crack-tip for steady-state interface crack propagation. Liu *et al.* [8] provided a more general higher-order asymptotic analysis for unsteady interface crack propagation that accounted for transient effects. They also conducted experiments to support the need of such an analysis. Tippur and Rosakis [9] performed the earliest experimental study on dynamic crack initiation and growth in bimaterials. Lee *et al.* [10] developed the field equations for an orthotropic bimaterial. Lee [11] subsequently developed the field equations for an isotropic-orthotropic bimaterial.

To date, work on isotropic-orthotropic bimaterials and interface fracture using strain gages is limited at best. Ricci *et al.* [12] used strain gages and photoelastic techniques to evaluate interface fracture parameters in bimaterials under quasi-static loads. Thus, this study focuses on developing strain field equations and critically examining them via experimentation to demonstrate the feasibility of the strain gage method.

## STRAIN FIELDS AROUND AN INTERFACIALLY PROPAGATING CRACK TIP

Crack growth along a bimaterial interface is generally referenced with respect to the material properties of the more compliant material, Material 1. (Material 2 is the stiffer material.) Crack propagation is considered subsonic for crack-tip velocities, $v$, below the shear wave velocity, $c_s$, of the more compliant material. From the governing equations for subsonic crack growth [5], the crack-tip stress field was found to be a coupled oscillatory field scaled by the dynamic complex stress intensity factor (CSIF), $\mathbf{K^d}$:

$$\sigma_{ij} = \frac{Re\left\{K^d\, r^{i\varepsilon(v)}\right\}}{\sqrt{2\pi r}}\,\tilde{\sigma}^1{}_{ij}(\theta, v) + \frac{Im\left\{K^d\, r^{i\varepsilon(v)}\right\}}{\sqrt{2\pi r}}\,\tilde{\sigma}^2{}_{ij}(\theta, v) \tag{1}$$

where $r$, $\theta$ are polar coordinates of a coordinate system translating with the crack tip at speed $v$, $\mathbf{K^d} = K_1{}^{\mathrm{d}} + iK_2{}^{\mathrm{d}}$ is the dynamic CSIF, and $\tilde{\sigma}^1{}_{ij}$ and $\tilde{\sigma}^2{}_{ij}$ are real, dimensionless angular functions [5]. The oscillatory index $\varepsilon$, which is the dynamic material mismatch parameter, is a function of crack tip speed ($\varepsilon = \varepsilon(v)$):

$$\varepsilon = \frac{1}{2\pi} \ln \frac{1-\beta}{1+\beta} \tag{2}$$

where, $\beta$ is the generalized Dundurs' parameter [7,8].

Using existing field equations for subsonic crack propagation in an isotropic-orthotropic bimaterial [11], the strain field equations were developed. For the orthotropic material (Material 2):

$$\begin{aligned}(\varepsilon_x)_2 = {} & \frac{K_I}{2\sqrt{2\pi r}D_2\cosh(\varepsilon\pi)}\left\{p_l\left[e^{-\varepsilon(\pi+\theta_l)}\overline{A_2}\cos\left(\varepsilon\ln\frac{r_l}{a}-\frac{\theta_l}{2}\right)+e^{\varepsilon(\pi+\theta_l)}A_2\cos\left(\varepsilon\ln\frac{r_l}{a}+\frac{\theta_l}{2}\right)\right]f_l(\theta) - p_s\left[e^{-\varepsilon(\pi+\theta_s)}\overline{B_2}\cos\left(\varepsilon\ln\frac{r_s}{a}-\frac{\theta_s}{2}\right)+e^{\varepsilon(\pi+\theta_s)}B_2\cos\left(\varepsilon\ln\frac{r_s}{a}+\frac{\theta_s}{2}\right)\right]f_s(\theta)\right\} \\ & + \frac{K_{II}}{2\sqrt{2\pi r}D_2\cosh(\varepsilon\pi)}\left\{-p_l\left[e^{\varepsilon(\pi+\theta_l)}\overline{A_2}\sin\left(\varepsilon\ln\frac{r_l}{a}-\frac{\theta_l}{2}\right)+A_2\sin\left(\varepsilon\ln\frac{r_l}{a}+\frac{\theta_l}{2}\right)\right]f_l(\theta) + p_s\left[e^{-\varepsilon(\pi+\theta_s)}\overline{B_2}\sin\left(\varepsilon\ln\frac{r_s}{a}-\frac{\theta_s}{2}\right)+B_2\sin\left(\varepsilon\ln\frac{r_s}{a}+\frac{\theta_s}{2}\right)\right]f_s(\theta)\right\}\end{aligned} \tag{3a}$$

$$\begin{aligned}(\varepsilon_y)_2 = {} & \frac{K_I}{2\sqrt{2\pi r}D_2\cosh(\varepsilon\pi)}\left\{pq_l\left[e^{-\varepsilon(\pi+\theta_l)}\overline{A_2}\cos\left(\varepsilon\ln\frac{r_l}{a}-\frac{\theta_l}{2}\right)+e^{\varepsilon(\pi+\theta_l)}A_2\cos\left(\varepsilon\ln\frac{r_l}{a}+\frac{\theta_l}{2}\right)\right]f_l(\theta) - qq_s\left[e^{-\varepsilon(\pi+\theta_s)}\overline{B_2}\cos\left(\varepsilon\ln\frac{r_s}{a}-\frac{\theta_s}{2}\right)+e^{\varepsilon(\pi+\theta_s)}B_2\cos\left(\varepsilon\ln\frac{r_s}{a}+\frac{\theta_s}{2}\right)\right]f_s(\theta)\right\} \\ & + \frac{K_{II}}{2\sqrt{2\pi r}D_2\cosh(\varepsilon\pi)}\left\{-pq_l\left[e^{-\varepsilon(\pi+\theta_l)}\overline{A_2}\sin\left(\varepsilon\ln\frac{r_l}{a}-\frac{\theta_l}{2}\right)+A_2\sin\left(\varepsilon\ln\frac{r_l}{a}+\frac{\theta_l}{2}\right)\right]f_l(\theta) + qq_s\left[e^{-\varepsilon(\pi+\theta_s)}\overline{B_2}\sin\left(\varepsilon\ln\frac{r_s}{a}-\frac{\theta_s}{2}\right)+B_2\sin\left(\varepsilon\ln\frac{r_s}{a}+\frac{\theta_s}{2}\right)\right]f_s(\theta)\right\}\end{aligned} \tag{3b}$$

$$\begin{aligned}(\gamma_{xy})_2 = {} & \frac{K_I a_{66}}{4\sqrt{2\pi r}D_2\cosh(\varepsilon\pi)}\left\{\alpha_l\left[e^{-\varepsilon(\pi+\theta_l)}\overline{A_2}\sin\left(\varepsilon\ln\frac{r_l}{a}-\frac{\theta_l}{2}\right)-e^{\varepsilon(\pi+\theta_l)}A_2\sin\left(\varepsilon\ln\frac{r_l}{a}+\frac{\theta_l}{2}\right)\right]f_l(\theta) - \alpha_s\left[e^{-\varepsilon(\pi+\theta_s)}\overline{B_2}\sin\left(\varepsilon\ln\frac{r_s}{a}-\frac{\theta_s}{2}\right)-e^{\varepsilon(\pi+\theta_s)}B_2\sin\left(\varepsilon\ln\frac{r_s}{a}+\frac{\theta_s}{2}\right)\right]f_s(\theta)\right\} \\ & + \frac{K_{II}a_{66}}{4\sqrt{2\pi r}D_2\cosh(\varepsilon\pi)}\left\{\alpha_l\left[e^{-\varepsilon(\pi+\theta_l)}\overline{A_2}\cos\left(\varepsilon\ln\frac{r_l}{a}-\frac{\theta_l}{2}\right)-e^{\varepsilon(\pi+\theta_l)}A_2\cos\left(\varepsilon\ln\frac{r_l}{a}+\frac{\theta_l}{2}\right)\right]f_l(\theta) - \alpha_s\left[e^{-\varepsilon(\pi+\theta_s)}\overline{B_2}\cos\left(\varepsilon\ln\frac{r_s}{a}-\frac{\theta_s}{2}\right)-e^{\varepsilon(\pi+\theta_s)}B_2\cos\left(\varepsilon\ln\frac{r_s}{a}+\frac{\theta_s}{2}\right)\right]f_s(\theta)\right\}\end{aligned} \tag{3c}$$

where the coefficients, defined by Lee [11], are given as

$$A_2 = \alpha_S + (1+M_a)\eta\ ,\ \overline{A_2} = \alpha_S - (1+M_a)\eta$$
$$B_2 = \alpha_l + (1+M_a)\eta\ ,\ \overline{B_2} = \alpha_l - (1+M_a)\eta$$

Eqn. 3 completely describes the two-dimensional strain field for the orthotropic half and were used in a parametric study of the strains near the interfacial crack tip. To determine the strain at a gage rotated $\theta_g$ degrees from the x-axis, a coordinate transformation is done accordingly:

$$\varepsilon_{x'x'} = \varepsilon_{xx}\cos^2\theta_g + \varepsilon_{yy}\sin^2\theta_g + \gamma_{xy}\cos\theta_g\sin\theta_g \tag{4}$$

Eqn. 4 may be rewritten in terms of $K_1^d$ and $K_2^d$. Then, substituting for the coefficients of $K_1^d$ and $K_2^d$ as $C_1$ and $C_2$, respectively, yields

$$\varepsilon_{x'x'} = C_1\left(\varepsilon, r, \theta, \theta_g, v\right)K_1^d - C_2\left(\varepsilon, r, \theta, \theta_g, v\right)K_2^d \tag{5}$$

The strain equations have three unknowns: $K_1^d$, $K_2^d$, and velocity $v$. The velocity is obtained experimentally by taking crack-tip position with respect to time; this is discussed below in the experiment section of this paper. The remaining two unknowns then require two strain measurements taken at the same time. Then, Eqn. 5 can be solved for $K_1^d$ and $K_2^d$ from two measured strains, $\varepsilon^{(1)}$ and $\varepsilon^{(2)}$; the superscript indicates the gage. Thus, the components of the complex stress intensity factor, $K_1^d$ and $K_2^d$, are given as

$$K_1^d = \frac{C_2^{(2)}\varepsilon^{(1)} - C_2^{(1)}\varepsilon^{(2)}}{C_2^{(2)}C_1^{(1)} - C_2^{(1)}C_1^{(2)}} \qquad K_2^d = \frac{C_1^{(2)}\varepsilon^{(1)} - C_1^{(1)}\varepsilon^{(2)}}{C_2^{(2)}C_1^{(1)} - C_2^{(1)}C_1^{(2)}} \tag{6}$$

## PARAMETRIC INVESTIGATION

A parametric study was conducted to understand the development of the strain field close to the crack tip. Subsequently, this information was used to optimize the location and orientation of the strain gages for the development of strain gage techniques used in this study to obtain the dynamic complex stress intensity factor $\mathbf{K^d}$ from a propagating interfacial crack.

### *Strain Gage Location*

The effect of the dynamic CSIF, $\mathbf{K^d}$, on the strain fields was examined to determine the optimum locations for the strain gages. The bimaterial system chosen for this parametric study was PSM-1 polycarbonate and Scotchply 1002 unidirectional, glass-fiber-reinforced, epoxy composite. This bimaterial has a relatively high material mismatch, $\varepsilon$, on the order of 0.12. The material properties are given in Table 1. Also, it is noted that the fiber orientation angle, $\alpha$, is the angle between the fiber direction and the x-axis (i.e. the interface).

TABLE 1
MECHANICAL PROPERTIES USED IN BIMATERIAL SPECIMENS

| **Property** | **PSM-1*** | **Scotchply® 1002**** |
|---|---|---|
| Young's Modulus, E (GPa) | 2.76 | $E_L = 30$<br>$E_T = 7.0$ |
| Poisson's Ratio, ν | 0.38 | $\nu_{LT} = 0.25$ |
| Density, $\rho$ (kg/m$^3$) | 1200 | 1860 |
| Material Fringe Value, $f_\sigma$ (kN/m/fringe) | 7.0 | |

* Manufactured by Measurements Group, Raleigh, NC, USA
** 3M® unidirectional, glass-fiber-reinforced epoxy

Since the crack travels along the interface, the position of the gages would be set at a distance of one half the plate thickness ($y \geq 0.5B$) from the interface. This satisfies the plane stress condition as well as avoids difficulties introduced by the plastic zone at the crack tip. This would also ensure that the gages would be within the singularity-dominated region such that the singular strain field solutions are valid.

### *Effects of Mixity and Velocity on the Strain Gage Orientation*

Eqn. 4 above was used to study the strain fields around a propagating interfacial crack. To determine the optimal strain gage orientation angle, $\theta_g$, a method was developed to examine the theoretical strain profiles of an interfacially propagating crack as sensed by a nearby strain gage. The strain gage profiles would be compared for various gage angles over suitable mixity, $\phi$, and velocity, $v$, domains. (*Mixity* is the relative

strength $K_2^d$ to $K_1^d$.) For given values of mixity and velocity, it was noted that, as $\theta_g$ was changed, the peak of the strain profile relative to the gage would shift along the interface (i.e. the x-axis). In this case, the coordinate system is fixed with respect to the gage with the y-axis passing through the center of the gage (i.e. x = 0 is on the interface directly below the gage – referred to hereafter as the *gage datum*). The crack tip propagates along the interface in the positive x-direction. Thus, $\theta_g$ could be selected such that the peak strain occurs when the crack tip is at or very near gage datum. Figure 1 illustrates the crack-tip position at peak strain as a function of mixity for varying velocity for $\theta_g = 55^o$ and $\alpha = 0^o$.

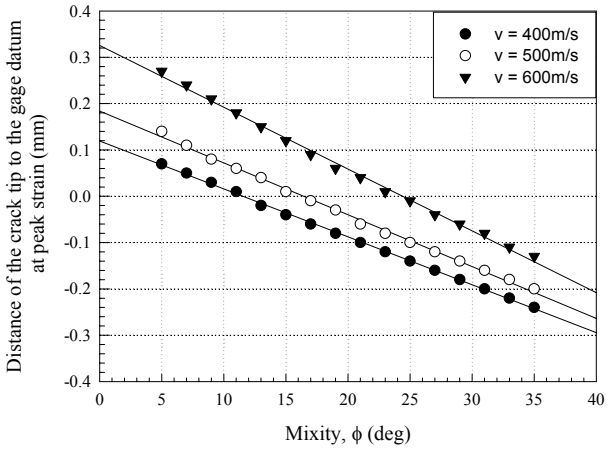


**Figure 1.** Location of crack tip relative to gage datum for varying mixity and velocity ($\theta_g = 55^o$; $\alpha = 0^o$).

For a given velocity, the crack tip position varies just 0.3 mm over the range of mixities. From preliminary model experiments, values for mixity were expected in the range of 10 to 30 degrees and velocity in the range of 500 to 600 m/s. That means the expected crack tip position would vary just 0.2 mm. It was further found that changes in $\theta_g$ result in the curves shifting significantly relative to gage datum. Thus, it is clear that the crack tip position is relatively insensitive to mixity and velocity and greatly influenced by $\theta_g$. For fiber orientation angle, $\alpha$, = $0^o$, $\theta_g$ is $55^o$, and for $\alpha$, = $90^o$, $\theta_g$ is $100^o$.

***Crack-Tip Position Uncertainty and Strain Error***

The error in the complex stress intensity components, $K_1^d$ and $K_2^d$, induced by an error in crack-tip position was investigated. By varying the crack-tip position from –1.0 to 1.0 mm around the gage datum, it was found that the variation in $K_1^d$ is less than two percent and for $K_2^d$ less than three percent. Ricci *et al*. [12] examined averaging error in the case of quasi-static loading as a function of radius and gage angle for various values of $K_1^d$ and $K_2^d$ for a Micromeasurements, Inc., USA, model CEA-06-015UW-120 strain gage, the same gage to be used in this study. It was found that for $r \geq 0.4B$, the averaging error was less than 0.2%. Similar error is assumed in the experiments herein.

## EXPERIMENTAL PROCEDURE

The parametric study was followed by experimentation, in which strain gage techniques were used to obtain values of $\mathbf{K}^d$ from a propagating crack as it passed a series of strain gages. Results from the strain gage data were then compared to results obtained from photoelastic data conducted as part of these experiments.

***Setup and Procedure***

Experiments were designed and conducted using a PSM-1/Scotchply single edge notch tension (SENT) bimaterial specimen, shown in Figure 2. Four strain gages were mounted on the Scotchply half at an angle of $55^o$ ($\alpha = 0^o$) or $100^o$ ($\alpha = 90^o$) and 5 mm above the interface. The gages were hooked up to a Lecroy high-

frequency digitizer, which recorded the interface fracture data at a rate of 1 MHz. The specimen was placed into a Vishay loading frame and loaded until fracture.

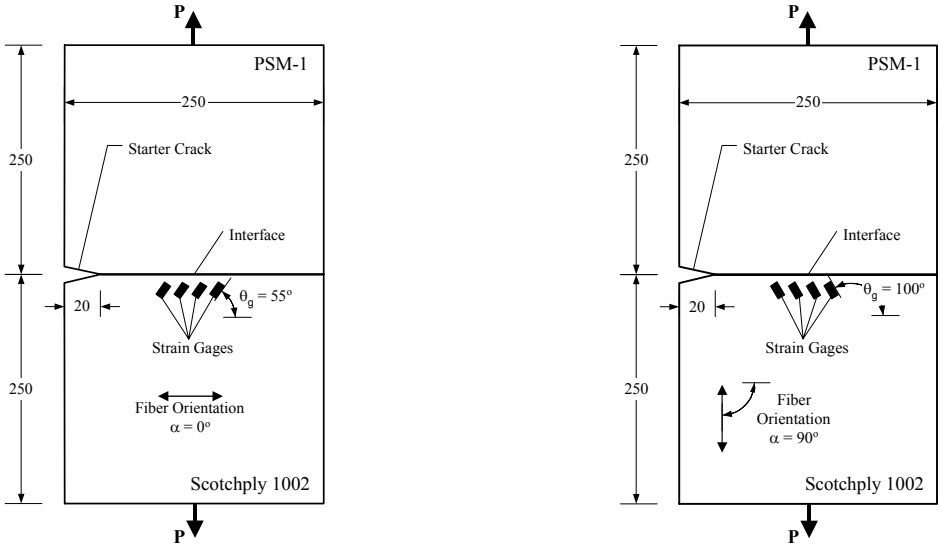


**Figure 2.** Single edge notch tension (SENT) bimaterial specimen: a) $\alpha = 0^o$ b) $\alpha = 90^o$.

## RESULTS AND DISCUSSION

Experiments were conducted on the PSM-1/Scotchply bimaterial specimen described above. Figure 3 shows the experimental data obtained from an $\alpha = 0^o$ experiment. Figure 3a shows the strain gage data: four pulses that correspond to the four gages as the crack passed by. Assuming that the peak strain occurs when the crack is at gage datum, the crack-tip velocity, $v$, was determined to be 600 m/s, leaving just two unknowns: $K_1^d$ and $K_2^d$. Figure 3b shows a frame of photoelastic data from the same experiment.

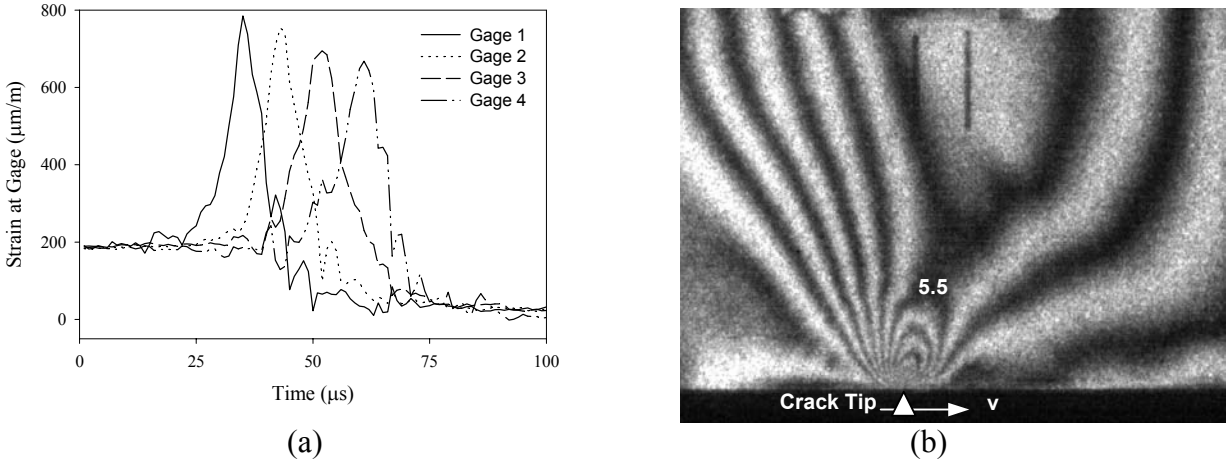


**Figure 3.** Experimental data from a propagating interfacial crack for $\theta_g = 55^o$ and $\alpha = 0^o$: a) Gage data showing strain pulses and b) Isochromatic fringes.

Using Eqn. 5, the strain gage data were analyzed to determine the magnitude of the CSIF. These values for $\mathbf{K^d}$ were compared to values obtained from photoelastic data for $\alpha = 0^o$ and $\alpha = 90^o$, shown in Figure 4a and 4b, respectively. There is reasonable correlation in the magnitude ($|\mathbf{K^d}| = \sqrt{\{(K_1^d)^2 + (K_2^d)^2\}}$)and trend of $\mathbf{K^d}$ for the strain gage results as compared to the photoelastic results. The strain gage analysis is a first-order

analysis based on the singular most term compared to a second-order photoelastic analysis. Thus, some error between the strain gage and the photoelasticity results is attributable to differences in the analyses.

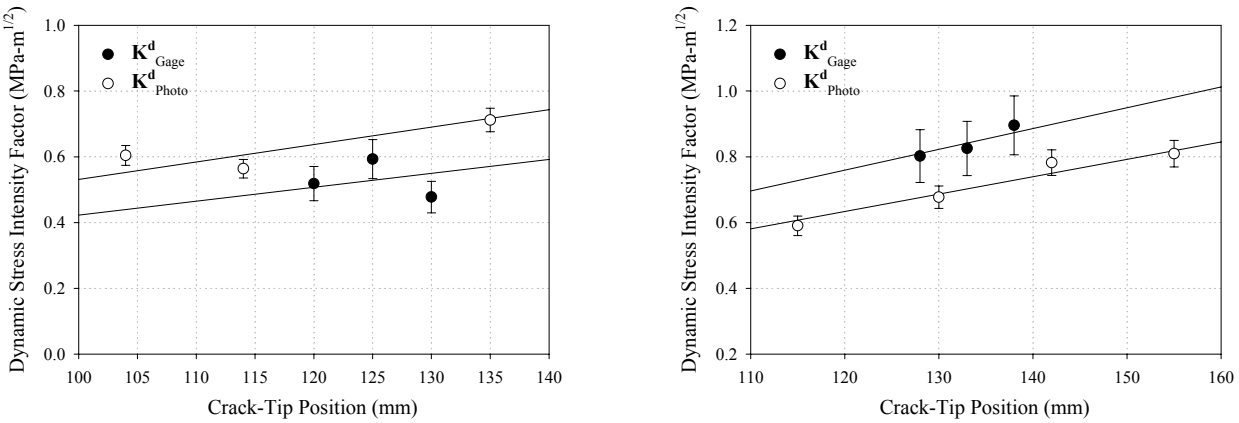


**Figure 4.** Dynamic Complex Stress Intensity Factor: a) $\alpha = 0^o$ b) $\alpha = 90^o$.

## CONCLUSION

An experimental study was conducted in which strain fields were developed and used to investigate the behavior of cracks propagating along the interface of an isotropic-orthotropic bimaterial. Analytical work focused on the influence of the dynamic CSIF, $\mathbf{K^d}$, on the strain field surrounding a crack tip, which yielded the optimum strain gage orientation. In the experimentation that followed, $\mathbf{K^d}$ for a PSM-1/Scotchply bimaterial was determined using strain gages. The trend and magnitude of $\mathbf{K^d}$ obtained from strain gage analysis compared favorably with those from photoelastic analysis from the same experiment. Thus, it is feasible to use strain gages to study subsonic interfacial crack propagation in isotropic-orthotropic bimaterials. Differences in the methods and analyses are the subject of an on-going study.

## ACKNOWLEDGEMENTS

The authors wish to acknowledge the support of the Naval Undersea Warfare Center ILIR, the Korean Science and Engineering Foundation (Grant No. 971-1003-017-2), and the National Science Foundation.

## REFERENCES

1. Dally, J. W. and Sanford, R. J. (1987) *Experimental Mechanics* **27**, 381-388.
2. Shukla, A., Agarwal, R. K., and Nigam, H. (1988) *Engineering Fracture Mechanics* **31**, 501-515.
3. Shukla, A., Agarwal, B. D., and Bhushan, B. (1989) *Engineering Fracture Mechanics* **32**, 469-477.
4. Khanna, S. K. and Shukla, A. (1994) *Engineering Fracture Mechanics* **47**, 345-359.
5. Yang, W., Suo, Z., and Shih, C.F. (1991) *Proceedings of the Royal Society* (London) **A433**, 679-697.
6. Deng, X. (1992) *Engineering Fracture Mechanics* **42**, 2, 237-242.
7. Deng, X. (1993) *Journal of Applied Mechanics* **60**, 183-189.
8. Liu, C., Lambros, J., and Rosakis, A. J. (1993) *Jour. of Mech. and Phys. of Solids* **41**, 2, 1887-1954.
9. Tippur, H. V. and Rosakis, A. J. (1991b) *Experimental Mechanics* **31**, 243-251.
10. Lee, K. H., Hawong, J. S., and Choi, S. H. (1996) *Engineering Fracture Mechanics* **53**, 1, 119-140.
11. Lee, K. H. (1999) *Korean Society of Mechanical Engineers Journal (A)* **23**, 9, 1463-1475.
12. Ricci, V., Shukla, A., and Singh, R. P. (1997) *Engineering Fracture Mechanics* **59**, 4, 273-283.